Cancer Cell International

RESEARCH

Open Access

Metformin regulates the proliferation and motility of melanoma cells by modulating the LINC00094/miR-1270 axis

Kuo-Wang Tsai[1,2], Jia-Bin Liao[3,4,5] and Hui-Wen Tseng[6,7,8,9*]

Abstract

Background Melanoma is an aggressive tumor with a high mortality rate. Metformin, a commonly prescribed diabetes medication, has shown promise in cancer prevention and treatment. Long noncoding RNAs (lncRNAs) are non-protein-coding RNA molecules that play a key role in tumor development by interacting with cellular chromatins. Despite the benefits of metformin, the anticancer mechanism underlying its effect on the regulation of lncRNAs in melanoma remains unclear.

Methods We investigated the lncRNA profiles of human melanoma cells with and without metformin treatment using a next-generation sequencing approach (NGS). Utilizing public databases, we analyzed the expression levels and clinical impacts of LINC00094 and miR-1270 in melanoma. The expression levels of LINC00094 and miR-1270 were verified in human cell lines and clinical samples by real-time PCR and in situ hybridization. The biological roles of LINC00094 and miR-1270 in cell growth, proliferation, cell cycle, apoptosis, and motility were studied using in vitro assays.

Results We identify a novel long noncoding RNA, namely LINC00094, whose expression considerably decreased in melanoma cells after metformin treatment. In situ hybridization analysis revealed substantially higher expression of LINC00094 in cutaneous melanoma tissue compared with adjacent normal epidermis and normal control tissues ($P < 0.001$). In nondiabetic patients with melanoma, the overall survival of high LINC00094 expression group was shorter than the low LINC00094 expression group with borderline statistical significance (log-rank test, $P = 0.057$). Coexpression analysis of LINC00094 indicated its involvement in the mitochondrial respiratory pathway, with its knockdown suppressing genes associated with mitochondrial oxidative phosphorylation, glycolysis, antioxidant production, and metabolite levels. Functional analysis revealed that silencing-LINC00094 inhibited the proliferation, colony formation, invasion, and migration of melanoma cells. Cell cycle analysis following LINC00094 knockdown revealed G1 phase arrest with reduced cell cycle protein expression. Combined TargetScan and reporter assays revealed a direct link between miR-1270 and LINC00094. Ectopic miR-1270 expression inhibited melanoma cell growth and motility while inducing apoptosis. Finally, through in silico analysis, we identified two miR-1270 target genes, CD276 and centromere protein M (CENPM), which may be involved in the biological functions of LINC00094.

Conclusions Overall, LINC00094 expression may regulate melanoma cell growth and motility by modulating the expression of miR-1270, and targeting genes of CD276 and CENPM indicating its therapeutic potential in melanoma treatment.

*Correspondence:
Hui-Wen Tseng
hwtseng6@gmail.com
Full list of author information is available at the end of the article

Introduction

Malignant melanoma is the most aggressive form of human skin cancer with early metastasis. Patients with end-stage melanoma typically have substantially low 5-year survival rates [1]. Over the preceding 3 decades, the incidence of melanoma has considerably increased worldwide. In patients with melanoma, tumorigenesis is a multistep process that involves the accumulation of multiple mutations, the occurrence of epigenetic alterations and transcriptomic aberrations, and the transformation of healthy melanocytes into melanoma cells [2]. One of the major challenges in managing patients with melanoma is the diverse mechanisms of treatment resistance, particularly in those with BRAF-mutated melanoma. Such therapeutic resistance develops through genetic mutation, overexpression, the activation or inhibition of effectors involved in cell signaling pathways, such as mitogen-activated protein kinase (MAPK), phosphoinositide 3-kinases (PI3K)/protein kinase B (AKT), and melanocyte Inducing Transcription Factor (MITF), or epigenetic factors at the cellular level [3].

Metformin is an oral antihyperglycemic agent that increases glucose tolerance in patients with type 2 diabetes mellitus (DM) by reducing their basal and postprandial plasma glucose levels. Metformin's primary mechanism of action relies on the modulation of cellular energy metabolism. Metformin exerts its glucose-lowering effect by inhibiting hepatic gluconeogenesis and the action of glucagon. It accomplishes this goal through a combination of mechanisms that are either dependent or independent on AMP-activated protein kinase (AMPK), particularly through the inhibition of mitochondrial respiration and mitochondrial glycerophosphate dehydrogenase and through a mechanism that involves lysosomes. Because metformin has a positive charge and because the membrane potential across the plasma membrane and mitochondrial inner membrane (positive outside) drives it into the cell and subsequently into the mitochondria, metformin accumulates within the mitochondria at concentrations of up to 1000 times higher than those in the extracellular medium [14, 15]. Among the actions of metformin, the most extensively studied mitochondrial action is the inhibition of Complex I in the respiratory chain, which inhibits the production of ATP [4]. This inhibition of Complex I in the mitochondria results in defective cAMP and protein kinase A signaling in response to glucagon. Therefore, understanding the primary mechanisms of metformin may aid in the development of novel treatments. Metformin may influence tumorigenesis either indirectly through the systemic reduction of insulin levels or directly through the induction of energetic stress.

MicroRNAs (miRNAs) and long noncoding RNAs (lncRNAs) are non-protein-coding RNA molecules that play a key role in tumor development by interacting with cellular chromatins and proteins to regulate genes involved in cell proliferation, motility, invasiveness, and angiogenesis [5]. In addition, lncRNAs serve as decoys to titrate cancer-related miRNAs and regulate the aforementioned cellular activities [6, 7]. They are also regarded as essential regulators of cancer progression. Notably, lncRNA dysregulation plays a key role in the carcinogenesis of melanoma. Dysregulated lncRNAs may regulate cancer cell growth, metastasis, or drug resistance. Multiple studies have indicated that many lncRNAs—including HOTAIR, BANCR, MALAT1, SPRY-IT1, and SMMSON—are dysregulated in melanoma [8]. Furthermore, some specific lncRNAs—including MIR31HG, MIR205HG, MIAT, NEAT1, MALAT1, HAND2-AS1, and H19—play a key role in the progression of melanoma [9–15]. According to Han et al. [16], downregulation of lncRNA TSLNC8 increases the resistance of melanoma to the BRAF inhibitor PLX4720 by binding with PP1α to reactivate MAPK signaling.

Long intergenic non-protein-coding RNA 94 (LINC00094; GeneCards symbol: BRD3OS; also known as BRD3 Opposite Strand) is found at the genomic location chr9q34.2. LINC00094 (BRD3OS) is associated with multiple diseases, including pulmonary squamous cell carcinoma (SCC). It is also downregulated in the pulmonary SCC tissues of smoking patients, with statistical analysis indicating an association between LINC00094 dysregulation and poor prognosis [17]. LINC00094 is a superenhancer-associated functional lncRNA that serves as a competing endogenous RNA (ceRNA) in esophageal SCC [18]. It is also one of the nine lncRNA signatures that predicts distant relapse-free survival in patients with HER2-negative breast cancer receiving taxane therapy and anthracycline-based neoadjuvant chemotherapy [19].

Despite the benefits of metformin, the anticancer mechanism underlying its effect on the regulation of lncRNAs in melanoma remains unclear. Accordingly, in this study, we used next-generation sequencing (NGS) to identify metformin-regulating lncRNAs in melanoma cells. We also examined the role of lncRNA-miRNAs (LINC00094/miR-1270) and relevant novel pathways in the proliferation and motility of a BRAF-mutated melanoma cell line after metformin treatment.

Materials and methods

Patient's sources

Human melanoma tissues were obtained from 112 pathological paraffin samples of patients who had undergone tumor resection at Kaohsiung Veterans General Hospital in Taiwan between October 1990 and October 2019.

In addition to these samples, basic information was obtained from the same hospital's department of pathology. Each sample, along with its basic information, was assigned a serial number without patient identification data. The inclusion criteria are described as follows: the patient shaving a pathological diagnosis of malignant melanoma, belonging to a specific stage of melanoma, and being 20 years of age or older. The exclusion criteria are described as follows: belonging to a certain vulnerable population, and insufficient paraffin samples. The study protocol was approved by the Institutional Review Board of Kaohsiung Veterans General Hospital (IRB approval No. VGHKS19-CT11-06). Malignant melanoma was staged in accordance with the TNM staging criteria established by the American Joint Committee on Cancer (2010). Data regarding patient demographics, risk factors, cancer cell pathological morphology, TNM stage, local and regional recurrence, distant metastasis, and survival status were obtained from the patients' hospital records. In addition, survival status was confirmed through hospital records. Overall survival (OS) was calculated as the date from the first pathological diagnosis of malignant melanoma to the date of all-cause mortality or that of the most recent follow-up.

In situ hybridization analysis (ISH) and grades of ISH expression

After each paraffin section underwent melanin bleaching, ISH was performed to determine the expression levels of LINC00094 in clinical human melanoma specimens, including tumor area, adjacent normal area, and normal control (nevus). Briefly, a DIG-labeled antisense probe was derived from a sequence of lncRNAs, with the expression level of an ISH probe used as a negative control. After hybridization, signals were detected using a polydetector system (BioTnA) per the manufacturer's instructions. Subsequently, slides were incubated with a mouse anti-DIG antibody for 1 h and washed with phosphate-buffered saline (PBS); this process was followed by the addition of mouse IgG horseradish peroxidase (HRP)-conjugated secondary antibodies at room temperature for 30 min. After the slides had been washed with PBS twice, DAB solution was added. Finally, DAB staining was used to obtain a signal. Analysis of the ISH expression of adjacent normal epidermis tissues with cutaneous melanoma and normal control (intradermal nevus) tissues was also conducted. The grades of ISH expression of cutaneous melanoma are described as follows: no dots (0), 1–3 dots/cell (1), 4–9 dots/cell (2), 10–15 dots/cell with < 10% cells in clusters (3), and > 15 dots/cell with > 10% cells in clusters (4). The area scores were categorized as follows: < 5% (0), 5%–25% (1), 26%–50% (2), 51%–75% (3), and 76%–100% (4). The expression level of each sample tissue was calculated as the sum of the grade score (0–4) and area score (0–4).

Cell lines with and without metformin treatment

Five human melanoma (A2058, A375, C32, RPMI7951 and MeWo) cell lines were obtained from the American Type Culture Collection and maintained on Dulbecco's modified Eagle's medium supplemented with 10% inactivated fetal bovine serum (Invitrogen, Carlsbad, CA, USA). Both the A2058, A375 and MeWo cell lines were treated with metformin at a concentration of 5 mmol/L for 4 days.

LncRNA profiles using next-generation sequencing

After melanoma cells had been cultured in the presence or absence of metformin for 4 days, total RNA was prepared using TRIzol (Invitrogen) per the manufacturer's protocol. RNA samples were processed using a strand-specific transcriptome preparation protocol and sequenced using an Illumina platform (Illumina, San Diego, CA, USA). Finally, the sequencing reads were mapped back to the human reference genome (hg19 from the UCSC) by using BLAT, with a minimum identity greater than 95%.

In silico data analysis in patients with melanoma

In this study, we performed an in silico analysis of lncRNA, miRNA and BRAF mutation, focusing on patients with melanoma. We used the Cancer Genome Atlas (TCGA) to obtain gene expression data for LINC00094 and miR-1270, along with clinical information from a cohort of patients with melanoma. A total of 458 patients with melanoma were included for analysis impacts on prognosis in this study. By using the Online consensus Survival webserver for Skin Cutaneous Melanoma (OSskcm) database [20], we analyzed the impacts of metformin-regulated lncRNAs on overall survival (OS) and disease-specific survival (DSS) of patients with melanoma. In addition, the status of BRAF mutation in melanoma and melanoma cell lines were obtained from cBioProtal for Cancer Genomic database.

RNAi knockdown of LINC00094 in melanoma cells

Melanoma cells were transfected with RNAi oligonucleotides directed against LINC00094 (Invitrogen), and random sequence siRNA oligonucleotides (Invitrogen) were used as a negative control. In this study, two siRNA were designed for targeting sequencing of LINC00094 (Figure S2). Real-time reverse transcription PCR (RT-PCR) was used 48 h after transfection to confirm the expression of LINC00094.

Cell migration and invasion assays

Cells were tested for their migration and invasion abilities in vitro in Transwell chambers (CoStar, Lowell, MA, USA). Either the lower side or the upper side of polycarbonate Transwell membranes (containing 8-μm pores) were coated with 50 μg/mL type I collagen or 80 μg/well Matrigel and used for migration or invasion assays, respectively. Cells were added to the upper chamber of a Transwell membrane. After incubation for 24 h at 37 °C, the cells on the lower side were prepared for Giemsa staining. The level of migration or invasion was determined using a microscope at 200× magnification. All experiments were repeated three times.

Cell proliferation and colony formation assays

To conduct a cell proliferation assay, 1×10^3 melanoma cells were seeded on a 96-well plate and transfected with LINC00094 siRNA (LINC00094-2 or si-LINC00094-3), miR-1270 mimics, or scramble control. Cell proliferation was evaluated on days 0, 1, 2, 3, and 4 by using a CellTiter-Glo One Solution Assay (Promega, Madison, WI, USA). All the experiments were independently repeated three times. To conduct a clonogenic assay, 1×10^3 live cells were deposited onto a six-well plate and transfected with LINC00094 siRNA (LINC00094-2 or si-LINC00094-3), miR-1270 mimics, or scramble control. After incubation at 37 °C for 2 weeks, cancer cell colonies were fixed with 3.7% formaldehyde for 10 min and stained with 0.2% crystal violet in 10% ethanol for 3 h. After the wells were rinsed with H_2O, they were air-dried. In each well, crystal violet was solubilized using 2 mL of 10% acetic acid, and the absorbance (optical density) of the solution was measured using a spectrophotometer at a wavelength of 620 nm.

Flow cytometry of cell cycle and apoptosis

After the cells were trypsinized, washed with PBS, resuspended in 70% ethanol, and maintained at 20 °C overnight, they were then centrifuged, washed with PBS, resuspended in 450 mL of PBS and 10 mL of 10 mg/mL DNase-free RNase (Roche Molecular Biochemicals), and incubated at 37 °C for 45 min. Following RNase treatment, 50 mL of propidium iodide (Boehringer Mannheim, Mannheim, Germany) was added, and the cells were incubated at room temperature for 10 min with light protection. Cell aggregates were removed through filtration before analysis. Cell cycle analysis was conducted using a Coulter EPICS XL flow cytometer.

Subcellular fraction localization

Nuclear and cytosolic fractions were separated using a PARIS kit (Life Technologies, Carlsbad, CA, USA) per the manufacturer's instructions. After RNA had been extracted using TRIzol (Invitrogen), 2 μg of total RNA was reverse-transcribed with random primers and SuperScript III Reverse Transcriptase (Invitrogen). Real-time PCR was then used to determine the expression level of lncRNA. U6 was used as a nuclear marker, and GAPDH was used as a cytosolic fraction marker.

Coexpression and pathway enrichment analysis

After the expression profiles of skin cutaneous melanoma (SKCM) were obtained from TCGA, gene correlation was calculated using Pearson's correlation coefficient. Multiple pathways were examined to determine the functions of LINC00094-related genes. Subsequently, the top 100 positively correlated and top 100 negatively correlated genes with LINC00094 were selected, and pathway enrichment analysis was conducted using g:Profiler and the DAVID and GSEA databases. In addition, the false-positive discovery rate was calculated using the FDR-corrected q value.

Western blot assay

After the cells were harvested at 24 h following transient transfection, they were washed with PBS; this process was followed by lysing with a lysis buffer (50 mM Tris–HCl at pH 8.0, 150 mM NaCl, 1% NP-40, 0.02% sodium azide, 1 μg/mL aprotinin, and 1 mM phenylmethylsulfonyl fluoride) at 4 °C for 30 min. Subsequently, the lysates were collected and centrifuged to remove cell debris, and protein assays were conducted using a Bio-Rad Protein Assay kit through a Bradford dye-binding procedure (Bio-Rad Laboratories, Hercules, CA, USA). After protein samples (60 μg) had been separated using sodium dodecyl sulfate polyacrylamide gel electrophoresis in 10% resolving gel with a Mini-PROTEAN 3 Cell apparatus, they were electrotransferred to nitrocellulose membranes (Amersham Pharmacia Biotech, Amersham, UK). After blocking at 4 °C overnight with PBS-Tween containing 5% skim milk, the membranes were incubated with primary antibodies for 1 h in PBS-Tween containing 5% skim milk. Subsequently, the membranes were incubated with anti-rabbit or mouse IgG HRP-conjugated secondary antibodies (1:10,000; Roche Molecular Biochemicals) for 1 h at room temperature. After washing three times with PBS-Tween, immunoreactive bands were detected using an Amersham ECL kit (Amersham Pharmacia Biotech).

Real-time RT-PCR

Total RNA (2 μg, DNase I treatment) was reverse-transcribed using oligo$(dT)_{15}$ primers and SuperScript III Reverse Transcriptase in accordance with the manufacturer's instructions (Invitrogen). After the reaction was performed in an incubator at 42 °C for 1 h, the enzyme

was inactivated through incubation at 85 °C for 5 min. Subsequently, cDNA was used for real-time PCR analysis with gene-specific primers, and gene expression was detected using a SYBR Green I assay (Applied Biosystems, Foster City, CA, USA). To determine the expression levels of lncRNAs by using a PCR thermocycler, the following PCR procedure was adopted: 94 °C for 10 min followed by 35 cycles at 94 °C for 1 min, 60 °C for 1 min, and 72 °C for 30 s, with a final extension at 72 °C for 10 min. GAPDH was used as an internal control. The sequences of the primers used in this study:

- LINC00094-F: CATTTGAATTCTCCAGCTGTGC
- LINC00094-R: TGCAAACAAGCCAGGACTCT
- GAPDH-F: TGCACCACCAACTGCTTAGC
- GAPDH-R: GGCATGGACTGTGGTCATGAG

Small RNA transcriptome extraction through NGS

RNA was extracted from three samples—namely A375 cells with LINC00094-2 knockdown, A375 cells with LINC00094-3 knockdown, and A375 control cells—with TRIzol (Invitrogen). A small RNA library was constructed using the method described in our previous study [21]. Sequencing was performed using a MiSeq V2 reagent kit (150 cycles; Illumina). Sequencing data were analyzed using our tool [22].

Stem–loop RT-PCR

For more details regarding this process, please refer to our previous study [23]. The expression levels of miR-1270 were normalized to those of U6 small RNA (ΔCt = target miRNA Ct − U6 Ct). The sequences of the primers used in this study:

- miR-1270-RT: CTCAACTGGTGTCGTGGAGTC GGCAATTCAGTTGAGACACAGCT
- miR-1270-GSF: CGGCGGCTGGAGATATGG AAGAG
- U6-F: CTCGCTTCGGCAGCACA
- U6-R: AACGCTTCACGAATTTGCGT

Identifying novel targets of miR-1270 in silico anaylsis

Using TargetScan and the miRDB databases, we identified putative target genes of miR-1270 through in silico analysis. By combining the top 100 predicted targets from each tool, we identified 22 genes predicted by both TargetScan and miRDB. To refine the identification of miR-1270 targets, we further analyzed the correlation between miR-1270 expression and these 22 genes in melanoma. Expression profiles of miR-1270 and the target genes were obtained from the TCGA database, and Pearson correlation coefficients were calculated for miR-1270 and target gene pairs. Since miRNAs typically regulate target gene expression negatively, an inverse correlation between miR-1270 and its targets is expected. Thus, a negative correlation coefficient was used as a reliable indicator for identifying miRNA-target gene pairs [24].

Ectopic expression of miR-1270

Ectopic expression of miR-1270 was induced in melanoma cells through transfection by 10 nM miRNA mimics (GenDiscovery Biotechnology, New Taipei City, Taiwan) with a Lipofectamine RNAiMAX reagent (Invitrogen). After 48 h of transfection, the expression levels of miR-1270 were analyzed using stem–loop real-time quantitative PCR.

Luciferase reporter assay

Briefly, sequences of LINC00094 were cloned into a pMIR-REPROT vector (AM5795; Thermo Fisher Scientific, Waltham, MA, USA). Subsequently, the pMIR-REPROT-LINC00094 vector was cotransfected with or without miR-1270 mimics into an A2058 cell line by using Lipofectamine 2000 (Invitrogen, Thermo Fisher Scientific). After 48 h of transfection, cell lysates were used to measure luciferase activity on a Dual-Glo Luciferase Assay System (Promega).

RNA chromatin immunoprecipitation assay

Briefly, an RNA chromatin immunoprecipitation assay was performed using an RNA-binding protein immunoprecipitation kit (Millipore, Billerica, MA, USA) to examine the interaction between LINC00094 and miR-1270. A2058 cells were transfected with miR-1270 mimics or scramble control for 48 h and lysed with a radioimmunoprecipitation assay buffer. The cell lysate was supplemented with Dynabeads M-280 Streptavidin (Invitrogen) conjugated with an anti-Ago1/2/3 or anti-IgG antibody. Finally, Ago2-bound RNA was extracted using TRIzol, and the levels of purified RNAs were determined using real-time quantitative PCR.

Statistical analysis

The Mann–Whitney U tests and the Kruskal–Wallis one-way ANOVA tests were employed to evaluate the correlations of lncRNA expression in melanoma tissues, adjacent normal tissues, and normal control tissues (nevi) with clinicopathological parameters. These clinicopathological parameters were defined at the time of initial diagnosis or surgery. OS was measured as the time from the initial surgery of the primary tumor to the date of death or that of the most recent follow-up. Cumulative survival curves were estimated using the Kaplan–Meier

survival method and compared using a log-rank test. A two-tailed p value lower than 0.05 was considered statistically significant.

Results

Identifying metformin-regulated lncRNAs through NGS

In a previous study [25], we reported that metformin strongly inhibited the growth and migration of melanoma cells by modulating the miR-192-5p-EPEMP1 and miR-584-3p-SCAMP3 axes. In the present study, to determine the role of lncRNAs in metformin-suppressed cell growth, we analyzed the RNA transcriptome profiles of A2058 and A375 cells treated with and without 5 mM of metformin through an NGS approach. After NGS, we collected more than 89 million clean reads from all libraries (Figure S1A). After dividing these clean reads into multiple categories depending on NCBI human reference genes, we discovered that more than 90% of the reads could be mapped (Figure S1A). Numerous lncRNAs were detected, but only a small fraction were identified as differentially expressed (fold change greater than 2 or less than 0.5) in melanoma cells treated with metformin compared to the control group (Figure S1B). The Venn diagram illustrates that 41 upregulated lncRNAs and 14 downregulated lncRNAs were concurrently identified in two melanoma cell lines (A2058 and A375) following metformin treatment (Fig. 1A).

By using the OSskcm database, we examined the association between the expression level of metformin-regulated lncRNA and the overall survival (OS) and disease-specific survival (DSS) of patients with melanoma. Among these metformin-regulated lncRNAs, only five lnsRNAs expression (LINC00189, CD27-AS1, PPP1R26-AS1, GDNF-AS1 and LINC00094) were significantly associated with prognosis of patients with melanoma. As shown in Fig. 1B, C, higher expression levels of LINC00094 and PPP1R26-AS1 were significantly associated with shorter OS in patients with cutaneous melanoma. By contrast, higher expression levels of GDNF-AS1, CD27-AS1, and LINC00189 were significantly associated with longer OS and disease-free survival (DFS) in patients with cutaneous melanoma.

Suppression of LINC00094 may contribute to metformin-induced inhibition of melanoma cell growth

In this study, LINC00094 was selected as a metformin-suppressed lncRNA to investigate its specific role in melanoma. The expression levels of LINC00094 were significantly reduced in BRAF-mutant melanoma cells (A2058 and A375) after 4 days of metformin treatment (Fig. 1D). A similar result was observed in the BRAF wild-type melanoma cell line, MeWo, indicating that metformin suppresses LINC00094 expression in both BRAF-mutant and wild-type melanoma cells (Fig. 1D). To confirm role of LINC00094 in metformin-induced suppression of melanoma cell growth, we examined the effects of metformin treatment in A2058 cells with ectopic overexpression of LINC00094. First, we induced LINC00094 overexpression in A2058 cells via transfection with the pLINC00094 expression vector. As shown in Figure S2B, C, LINC00094 expression levels were significantly elevated in A2058 cells with stable pLINC00094 expression compared to the control group. Notably, metformin-induced inhibition of A2058 cell proliferation was partially reversed (Figure S2C). These results suggest that metformin's inhibition of A2058 cell growth is partially mediated through a LINC00094-regulated signaling pathway.

Role of LINC00094 in the regulation of energy metabolic pathways through mitochondrial dysfunction

To understand the putative biological function of LINC00094, we conducted a coexpression analysis involving skin cutaneous melanoma (SKCM) RNA sequencing data obtained from TCGA. The top 100 positive and top 100 negative coexpression genes of LINC00094 through Pearson's correlation analysis were identified (Figure S3A). Pathway enrichment analysis revealed that LINC00094 presumably played a key role in energy metabolism and mitochondrial dysfunction, including transport-coupled proton, respiratory electron transport, mitochondrial crista formation, hydrogen ion transmembrane transport, ATP synthesis, purine ribonucleoside triphosphate metabolism, aerobic respiration, inner mitochondrial membrane organization, oxidative phosphorylation (OXPHOS), and aerobic respiration pathways (Figure S3B, C). According to previous studies [26–28], mitochondrial membrane potential (MMP) dissipation may result from severe energy deficiency, leading to cellular necrosis or even death. Therefore, MMP dissipation may be accompanied by cell growth inhibition and apoptosis, although this causal relationship remains to be elucidated.

Association between LINC00094 expression and poor prognosis

Using OSskcm database for stratification analysis, higher expression levels of LINC00094 were significantly associated with shorter OS (crude hazard ratio [CHR] = 2.4904, $p < 0.01$) and DFS (HR = 2.523, $p < 0.01$) in melanoma patients with stage I. However, in patients with stage II, III, or IV melanoma, such associations were not observed (Fig. 1E, F). To further determine the effect of LINC00094 expression on the prognosis of patients with melanoma, we examined the expression of LINC00094 by using an in situ hybridization (ISH)

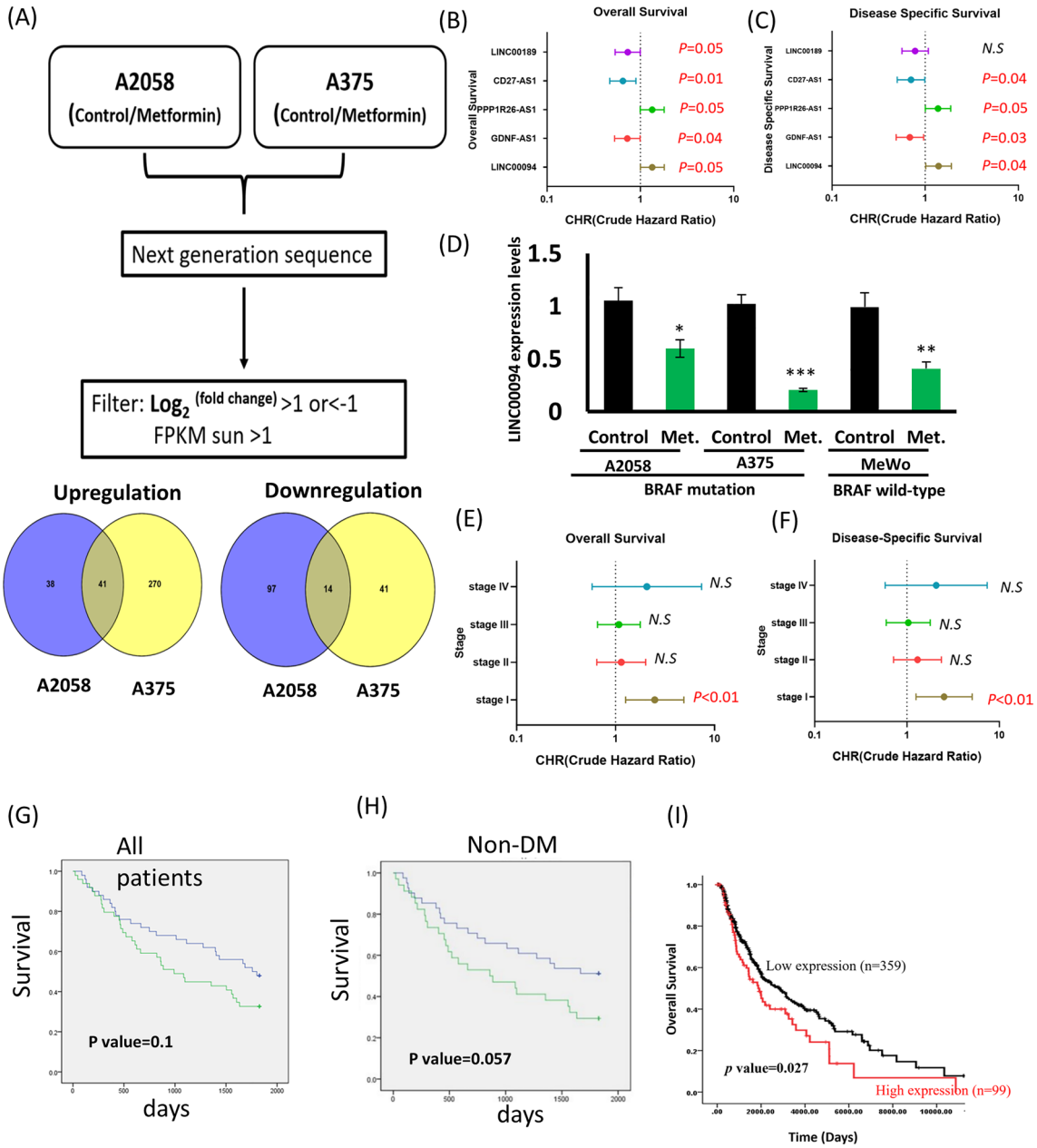

Fig. 1 Transcriptome profiles of melanoma cells with and without metformin treatment. **A** Flowchart depicting the identification process of differentially expressed genes through NGS in two melanoma cell lines with and without metformin treatment. In this process, lncRNAs with differential expression in melanoma cells were filtered at a fold change of ≥ 2 or < 0.5. The figure shows Venn diagrams of the numbers of upregulated and downregulated lncRNA candidates in the two melanoma cell lines with and without metformin treatment. **B**, **C** OS and DSS curves of metformin-suppressed lncRNAs selected and analyzed using Kaplan–Meier survival analysis from the OSskcm database (http://bioinfo.henuedu.cn/Melanoma/MelanomaList.jsp). **D** Expression levels of LINC00094 in A375, A2058 and MeWo cells with and without metformin treatment for 4 days. The BRAF mutation status was obtained from the cBioPortal database. **E**, **F** OS and DSS curves of metformin-upregulated lncRNA selected and analyzed using Kaplan–Meier survival analysis (stage I-IV) from the OSskcm database. **G** OS analysis of all included patients with melanoma was conducted using Kaplan–Meier survival analysis. **H** OS analysis of nondiabetic patients with melanoma was conducted using Kaplan–Meier survival analysis. **I** OS analysis of patients with melanoma (458 patients, TCGA) was conducted using Kaplan–Meier survival analysis

technique with skin paraffin sections of 112 patients with cutaneous melanoma. Table S1 presents the TNM stages of these 112 patients in detail. As indicated by the ISH results, LINC00094 was predominantly expressed in the cytoplasm of melanoma cells. In addition, the expression levels of LINC00094 (mean ± standard deviation

[SD] = 3.77 ± 2.3) were significantly higher in skin tissues with melanoma than in adjacent normal epidermis tissues (mean ± SD = 1.09 ± 1.37, $p < 0.001$) and normal control tissues (melanocytic nevus; mean ± SD = 1.33 ± 0.56, $p = 0.019$; Table 1). By contrast, no significant difference was observed between the expression levels of adjacent normal epidermis tissues (mean ± SD = 1.33 ± 0.56) and melanocytic nevus tissues (mean ± SD = 1.33 ± 0.56, $p = 0.177$; Table 1).

A log-rank test was conducted to examine the association between the expression level of LINC00094 and the postoperative survival of patients with melanoma. Receiver operating characteristic (ROC) curve analysis was conducted to define a cutoff value for LINC00094 expression. Using this cutoff value (i.e., 3.2), we divided our study cohort into two groups: a high LINC00094 expression group and a low LINC00094 expression group. Kaplan–Meier survival analysis revealed that the high LINC00094 expression group exhibited shorter OS than did the low LINC00094 expression group, albeit without statistical significance ($n = 103$, log-rank test, $p = 0.1$; Fig. 1G).

Because LINC00094 is involved in energy metabolism (according to pathway enrichment analysis) and because the metabolism of glucose is impaired in patients with DM, a stratified analysis of the studied patients with and without DM (referred to as the DM group and non-DM group, respectively) was conducted. As shown in Fig. 1H, in the non-DM group, the OS of the high LINC00094 expression group was shorter than that of the low LINC00094 expression group, with borderline statistical significance (log-rank test, $p = 0.057$, $n = 75$). This borderline statistical significance presumably resulted from the small sample size. In addition, in the DM group, the OS of the high LINC00094 expression group was shorter after 750 days than that of the low LINC00094 expression group, albeit without statistical significance. In the DM group ($n = 20$, metformin/DM: 13/20 = 65%), the percentage of metformin treatment with high ISH expression (metformin/DM: 6/11 = 54.5%) was lower than that with low ISH expression (metformin/DM: 7/9 = 77.7%; log-rank test, $p = 0.818$). However, the sample size was too small. Therefore, metformin treatment presumably increased survival before 750 days and eliminated the effect of high LINC00094 expression; this finding merits further investigation.

To increase the robustness of our findings, we expanded our analysis by including the clinical data and LINC00094 expression levels of 458 patients with melanoma from The Cancer Genome Atlas (TCGA) database. At a cutoff value of 4.43 (determined using a ROC method), comparison of the high and low LINC00094 expression groups indicated that the OS of the high LINC00094 expression group was significantly shorter than that of the low LINC00094 expression group (crude hazard ration (HR) = 1.41, 95% confidence interval [CI] = 1.04–1.91, $p = 0.027$). Kaplan–Meier survival analysis revealed that higher expression levels of LINC00094 were significantly associated with shorter OS in patients with melanoma ($p = 0.027$, Fig. 1I). In addition, multivariable Cox regression analysis revealed that higher expression levels of LINC00094 were significantly associated with shorter OS in patients with melanoma (adjusted HR = 1.38, 95% CI = 1.02–1.88, $p = 0.036$; Table 2). Additionally, we retrieved the BRAF mutation status of melanoma patients from the cBioPortal database. By comparing the BRAF mutation status with LINC00094 expression levels, we found no significant difference in LINC00094 expression between BRAF wild-type and BRAF-mutated patients (Figure S4 and Table S2). These results suggest that BRAF mutation status does not influence LINC00094 expression. However, LINC00094 may still serve as a prognostic biomarker for OS in melanoma patients.

Melanoma with LINC00094 knockdown inhibits the proliferation and induces the apoptosis

In this study, we utilized five melanoma cell lines: A375, A2058, C32, RPMI 7951, and MeWo. Among these, four cell lines, A375, A2058, RPMI 795, and RPMI 7951, carry the BRAF V600E mutation, while the MeWo cell line possesses the wild-type BRAF gene. As shown in Fig. 2A, higher expression levels of LINC00094 were observed in A375, A2058, and MeWo melanoma cell

Table 1 The expressions levels of LINC00094 were analyzed between the cutaneous melanoma tissues, corresponding adjacent normal epidermis, and normal control (nevus) by in situ hybridization approach

Adjacent normal	Cutaneous melanoma	Normal control (nevus)	P-value
Mean ± SD	Mean ± SD	Mean ± SD	
(n = 87)	(n = 103)	(n = 6)	< 0.001
1.09 ± 1.37^{ab}	3.77 ± 2.3^{ac}	1.33 ± 0.56^{bc}	

p values were estimated by Kruskal–Wallis one-way ANOVA test

Statistical significance: a two-tailed P-value of <0.05

Mann–Whitney U test: [a]p < 0.001; [b]p = 0.177; [c]p = 0.019

Table 2 Univariate and multivariate Cox's regression analysis of LINC00094 expression for overall survival of patients with melanoma

Characteristic	No. (%)	OS			
		CHR (95% CI)	P-value	AHR (95% CI)	P-value
LINC00094	(n = 458)				
Low	359 (78.4)	1.00		1.00	
High	99 (21.6)	1.41 (1.04–1.91)	**0.027**	1.38 (1.02–1.88)	**0.036**

AHR were adjusted for AJCC pathological stage (II, III and IV vs. I)

Statistical significance (bold): a two-tailed P-value of <0.05

DSS disease-specific survival, *DFS* disease-free survival, *CHR* crude hazard ratio, *AHR* adjusted hazard ratio

lines, whereas lower expression levels were observed in C32 and RPMI7951 cells (Fig. 2A). Loss-of-function analysis of A375 and A2058 cells was conducted using individual small interfering RNAs (siLINC00094#2 and siLINC00094#3) transfection (Figure S4). Quantitative polymerase chain reaction (PCR) measurements revealed a significant reduction in the relative expression of si-LINC00094 in A2058 and A375 cells with si-LINC00094 transfection compared with the control group (Fig. 2B, C). Cell proliferation analysis revealed that LINC00094 knockdown reduced the cell proliferation and colony formation capabilities of A375 and A2058 melanoma cells (Fig. 2D–I). In addition, LINC00094 knockdown significantly reduced the migration and invasion capabilities of A375 and A2058 melanoma cells (Fig. 3A–D). Cell cycle distribution analysis of cell population after LINC00094 knockdown (Fig. 4A–D) revealed a significant increase in sub-G1 and G1 phase A2058 and A375 melanoma cells after 72 h of incubation, along with a significant decrease in S and G2/M phase cells. Finally, LINC00094 knockdown induced apoptosis in A2058 and A375 melanoma cells (Fig. 4E–H). According to the results of Western blot analysis for cell-cycle-related genes, A2058 and A375 melanoma cells with LINC00094 knockdown exhibited lower expression levels of CCND1, CDK4, E2F1, CCNA2, and CCNB1 but a higher expression level of P27 (Figure S5A); lower expression levels of pro-survival (Bad/p-Bad) and anti-apoptosis (Bcl-2) proteins (Figure S5B); and lower expression levels of PI3K and AKT (Figure S5C). In summary, LINC00094 knockdown inhibited the growth of melanoma cells by inhibiting the PI3K/AKT signaling pathway, thereby hindering cell cycle progression and inducing apoptosis.

LINC00094 modulates the growth of melanoma cells through miR-1270 sponging and target genes of CD276 and CENPM

To determine whether LINC00094 is expressed in the cytoplasm or nucleus, nuclear and cytoplasmic RNA extraction was conducted to isolate nuclear and cytoplasmic RNA, and real-time PCR was employed to confirm the expression levels. In A2058 cells, the relative expressions of LINC00094 were determined to be 65% in the cytoplasm and 35% in the nucleus, whereas in A375 cells, the relative expressions of LINC00094 were determined to be 60% in the cytoplasm and 40% in the nucleus. This distribution pattern closely resembled that of the relative expression of glyceraldehyde 3-phosphate dehydrogenase (GAPDH), which is predominantly expressed in the cytoplasm (Figure S6). These results indicated that LINC00094 was predominantly expressed in the cytoplasm of melanoma cells, suggesting a potential biological function involving the modulation of endogenous miRNA expression.

To functionally identify the novel miRNA associated with LINC00094, the upregulated miRNA transcriptome in A375 cells with si-LINC00094 transfection and the miRNA database obtained from TargetScan binding prediction for miRNA from LINC00094 were intersected. Only miR-1270 was detected as miRNA in the intersection between upregulated miRNA and TargetScan prediction miRNA from LINC00094 (Fig. 5A). Dual luciferase reporter assays revealed lower luciferase fluorescence activity in cells cotransfected with miR-1270 and LINC00094 compared with cells with empty vectors (Fig. 5B). Ago2 precipitation assays revealed an interaction between miR-1270 and LINC00094 within the Ago2 complex, with high coexpression of LINC00094 and miR-1270 in the cells (Fig. 5C, D).

In A2058 cells with LINC00094 knockdown, an increase in endogenous miR-1270 expression was observed (Fig. 5E, F). A reverse experiment revealed no significant change in the expression of LINC00094 in A2058 cells with miR-1270 mimic transfection (Fig. 5G, H). To determine the effect of miR-1270 on growth and colony formation, the functional role of miR-1270 in melanoma cells was extensively examined through miR-1270 mimic transfection. Similar to the effects observed with LINC00094 knockdown, the overexpression of miR-1270 significantly impeded the ability of melanoma cells

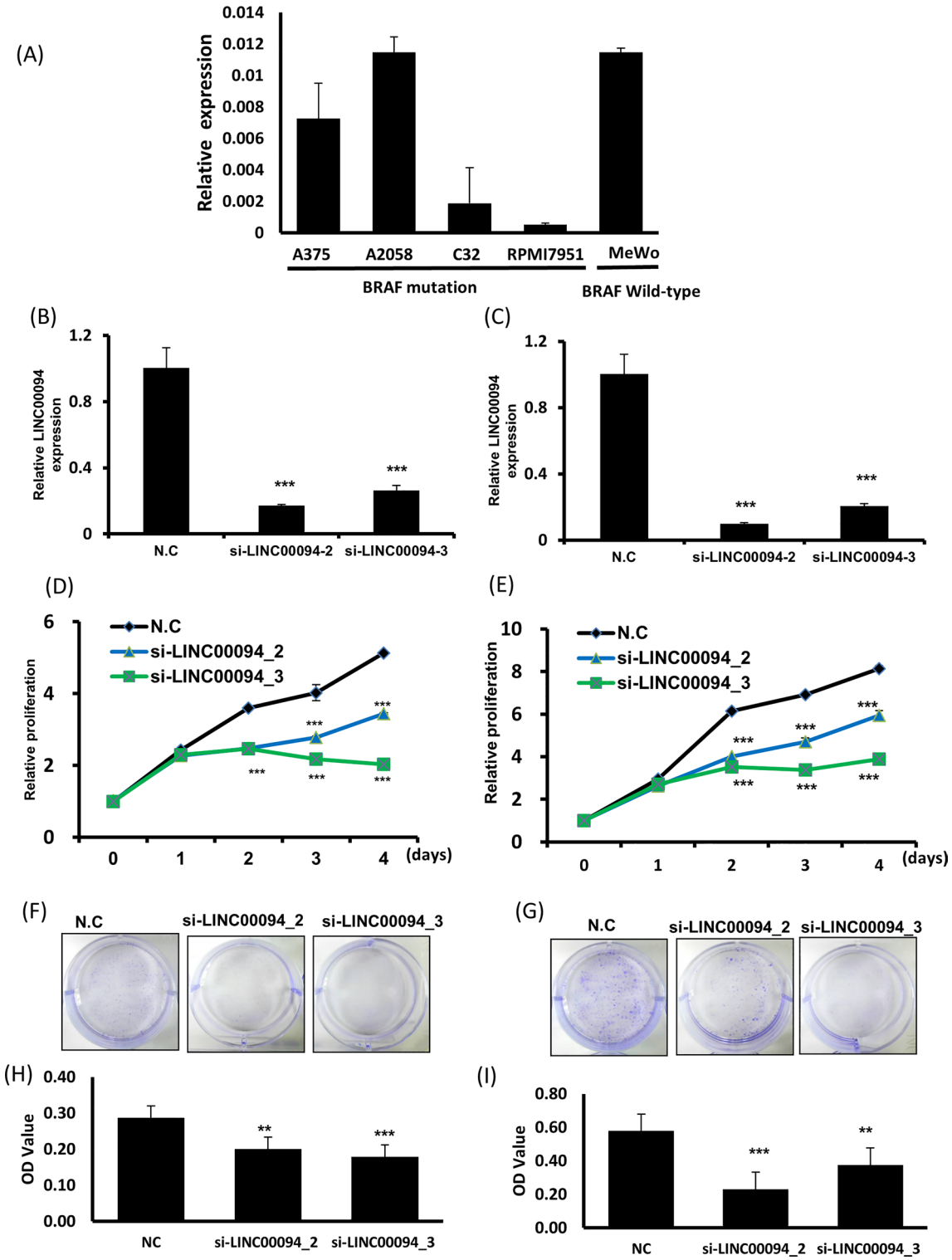

Fig. 2 Suppression of melanoma cell growth by LINC00094 knockdown. **A** Real-time PCR analysis of LINC00094 expression in five melanoma cell lines. The BRAF mutation status was obtained from the cBioPortal database. **B**, **C** Evaluation of LINC00094 expression in A2058 and A375 cells transfected with two siRNA (siLINC00094-2 and si-LINC00094-3) for 48 h. **D**, **E** Evaluation of cell proliferation in A2058 and A375 cells after LINC00094 knockdown. **F**, **G** Inhibition of colony formation ability in A2058 and A375 cells after LINC00094 knockdown. **H**, **I** Quantification of relative colony formation ability

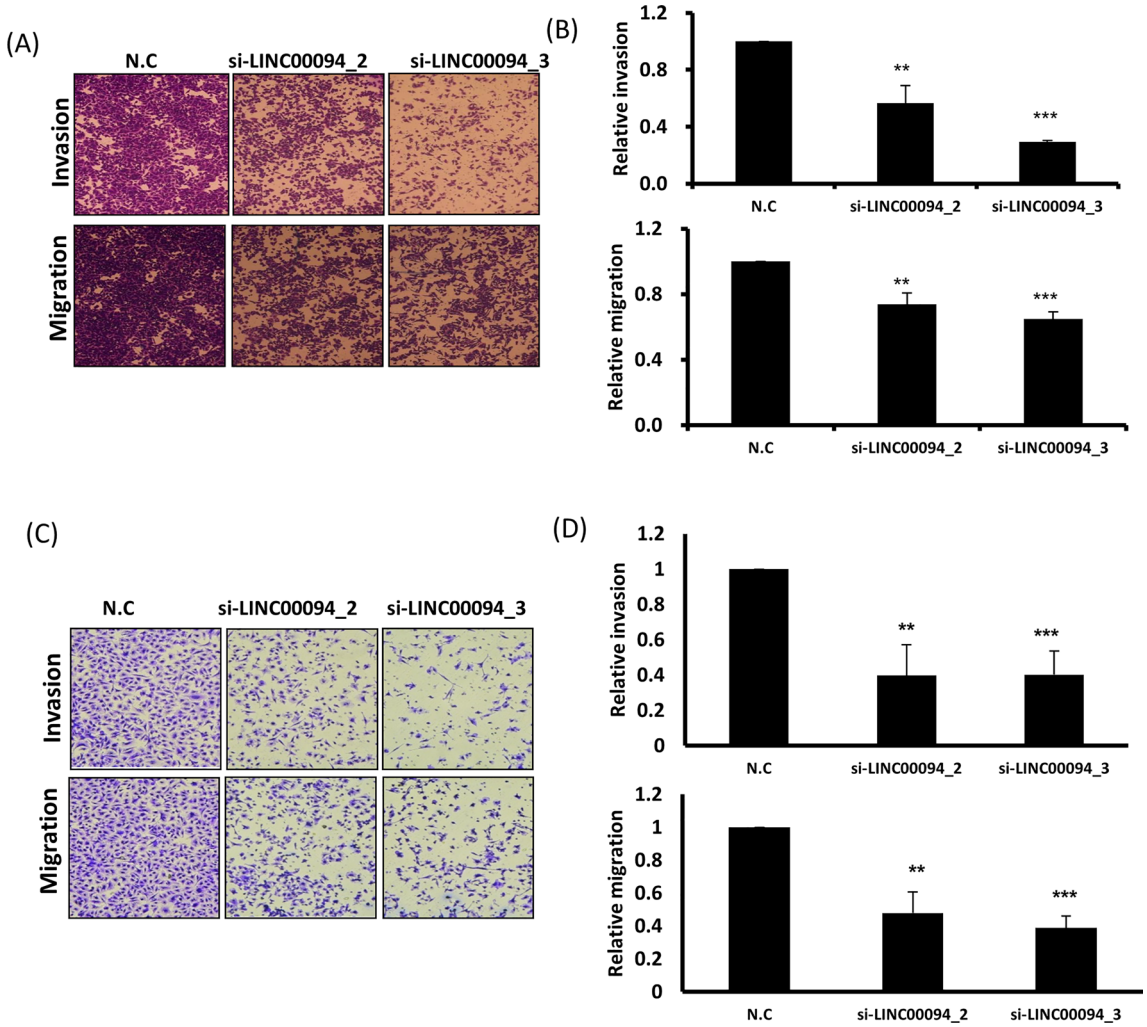

Fig. 3 Suppression of melanoma cell motility by LINC00094 knockdown. **A**, **B** Evaluation of the migration and invasion ability of A2058 cells after LINC00094 knockdown, followed by the quantification of their relative motility. **C**, **D** Evaluation of the migration and invasion ability of A375 cells after LINC00094 knockdown, followed by the quantification of their relative motility

to proliferate and form colonies (Fig. 6A–H). Cell cycle analysis revealed an increase in the percentage of cells in phases G1 and sub-G1, along with a decrease in the percentage of cells in phases S and G2/M (Fig. 7A–D). These findings strongly suggest that LINC00094 exerts its biological function by serving as a sponge for miR-1270 expression in melanoma cells.

To better understand the mechanism by which miR-1270 regulates melanoma cell function, we sought to identify its target genes. Through a literature search, we identified 15 previously reported miR-1270 targets across various cancer types, including lung [29, 30], hepatocellular [31–33], glioblastoma [34], osteosarcoma [35], ovarian [36, 37], thyroid [38], cervical [39, 40], and bladder cancers [41, 42] (Fig. 8A). These genes are known to be regulated by miR-1270 through directly binding to their 3′ UTR regions. However, the real relationship between miR-1270 and these target genes in melanoma remains unclear. If these miR-1270-target gene pairs play critical role in melanoma, we would expect a negative correlation between miR-1270 and its target gene expression [24]. To explore this, we analyzed expression profiles of miR-1270 and its 15 known target genes in melanoma using transcriptome data from the TCGA database. Our data revealed that CENPM expression exhibited a negative correlation with miR-1270 expression ($r = -0.182$) (Table S3 and Fig. 8B). In addition to the known targets, we identified novel potential targets of miR-1270 using prediction tools. By integrating the top 100 candidates from TargetScan and miRDB, we identified 22 putative

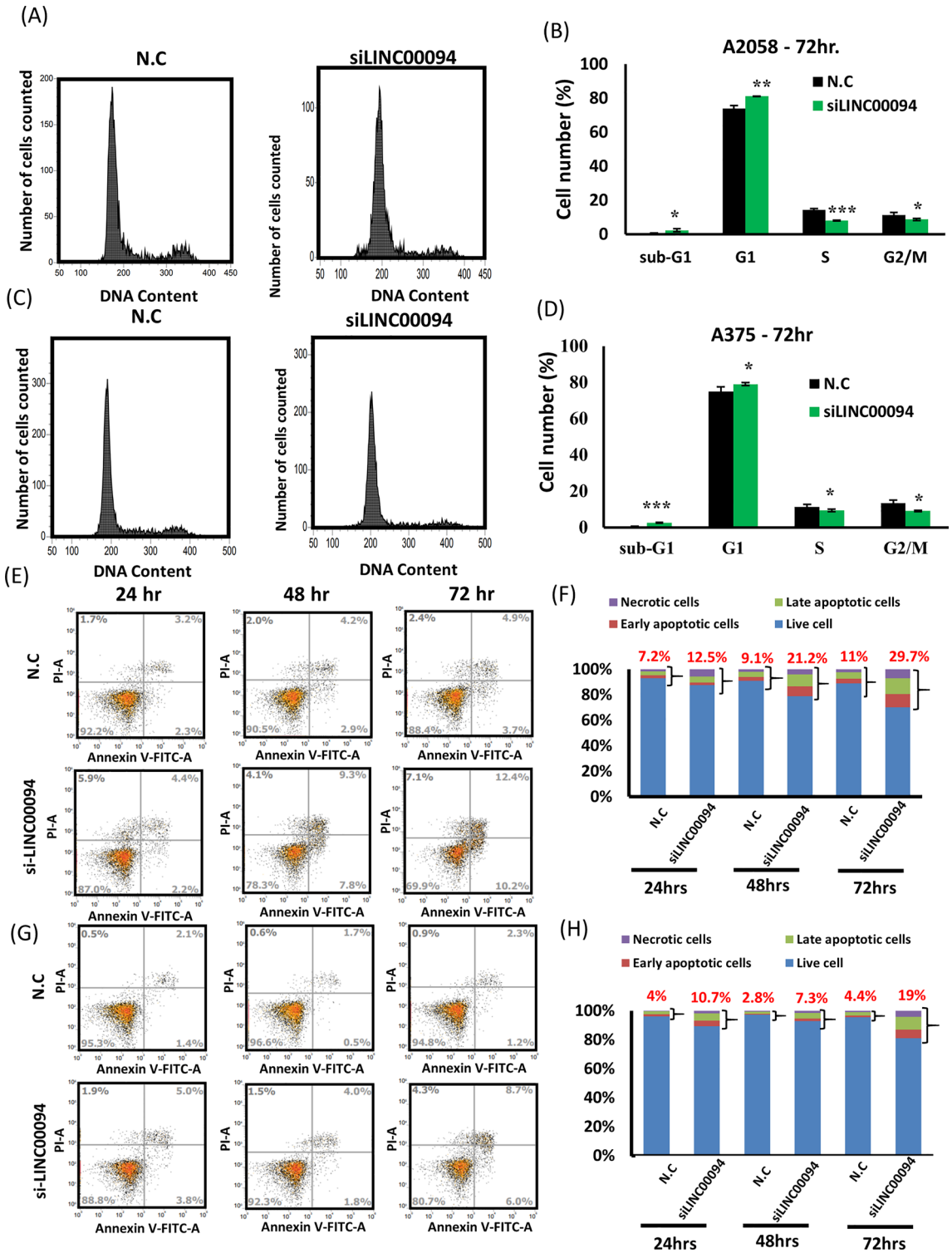

Fig. 4 Impaired cell cycle progression and induction of apoptosis by LINC00094 knockdown in melanoma cells. **A**, **B** Analysis of cell cycle distribution in A2058 cells with LINC00094 knockdown for 72 h. **C**, **D** Analysis of cell cycle distribution in A375 cells with LINC00094 knockdown for 72 h. **E**, **G** Evaluation of apoptosis in A2058 and A375 cells after LINC00094 knockdown for 24, 48, and 72 h. **F**, **H** Quantification of the percentage of apoptotic cells

miR-1270 targets (Fig. 8A). Pearson correlation analysis further revealed a negative correlation between miR-1270 and CD276 expression in melanoma cells ($r = -0.148$) (Fig. 8C). Previous studies have suggested that both CD276 and CENPM may have oncogenic roles in various cancers [43, 44]. In summary, we identified two miR-1270 target genes, CD276 and CENPM, which may contribute to metformin-induced growth suppression via modulation of the LINC00094/miR-1270 axis in melanoma.

Discussion

Patients with melanoma tend to develop regional lymph nodes or distant metastases. They also tend to develop resistance to some intensive treatments, including surgery, chemotherapy, electrotherapy, immunotherapy, and targeted therapy. Melanoma cells appear to immune escape from such treatments because they carry multiple potential gene mutations that are presumably attributable to different microenvironments [45, 46]. According to clinical studies and animal models, metformin, the first oral hypoglycemic agent of choice for type 2 DM, plays a role in the growth and treatment of certain melanoma cell lines [47]. In patients with diabetes, metformin reduces blood sugar without inducing hypoglycemia. Specifically, metformin reduces hepatic gluconeogenesis and increases the absorption of glucose by skeletal muscles [4, 48]. It also has an effect on mitochondria and thus requires the activation of metabolic checkpoint AMP-activated protein kinase (AMPK), which hinders protein synthesis and cell proliferation and inhibits the mammalian target of rapamycin complex 1 (mTORC1) [49, 50]. Multiple studies have indicated that acidosis-exposed environments may significantly increase the suppressive effect of metformin on the growth and motility of melanoma cells by inducing oxidative phosphorylation OXPHOS [51]. Urbonas et al. [52] reported that diabetic patients (type 2 DM) with melanoma who received metformin exhibited a lower risk of melanoma-specific mortality compared with nondiabetic patients; however, a previous clinical trial indicated that metformin monotherapy had no benefit for patients with melanoma of an advanced stage [53]. Previous studies have reported many potential links of genes, miRNAs, and lncRNAs with the progression and survival rate of melanoma, as well as a potential pathway involving metformin and melanoma. For instance, Tomic et al. [54] reported that metformin exerted an antiproliferative effect on melanoma cells, with normal human melanocytes being resistant to this metformin-induced effect. That study also indicated that metformin treatment in melanoma cells induced cell cycle arrest in phase G0/G1, thereby impairing tumor growth in mice. In addition, LC3 and ATG5 knockdown reduced the degree of apoptosis and inhibited the antiproliferative effect of metformin on melanoma cells, thereby inhibiting autophagy. Overall, metformin inhibited the proliferation of mouse melanoma B16 cells and induced their apoptosis, presumably by regulating the PI3K/AKT/mTOR signaling pathway [55].

Few studies have examined the role of LINC00094 in multiple types of cancer. Superenhancers play a role in tumorigenesis and regulate the expression of specific lncRNAs. Piipponen et al. [56] discovered that superenhancer-regulated LINC00094 upregulated the expressions of matrix metalloproteinase (MMP)-1 and MMP-13 and promoted the invasion of cutaneous SCC cells. That study also reported upregulated LINC00094 expression in cutaneous SCC cells and the downregulation of LINC00094 expression by SE inhibitors THZ1 and JQ1 through the MEK1/ERK1/2 pathway. In addition, that study reported higher BRD3OS (LINC00094) expression in cutaneous SCC cells and metastatic tumors compared with normal skin, actinic keratoses, and cutaneous SCC cells in situ. Therefore, those researchers concluded that BRD3OS (LINC00094) knockdown inhibited the production of MMP-1 and MMP-13 by cutaneous SCC cells and inhibited the growth of human cutaneous SCC xenografts in vivo. Xiang et al. [57] reported that the LINC00094/miR-19a-3p/CYP19A1 axis affected the degree of sensitivity to letrozole through the EMT pathway in estrogen-receptor-positive (ER-positive) breast cancer. The LINC00094 sponge adsorbed miR-19a-3p, which exhibited higher expression in the plasma of patients with breast cancer or ER-positive breast cancer compared with healthy individuals. The expression of miR-19a-3p also promoted the migration and EMT of breast cancer cells and reduced the sensitivity of breast

(See figure on next page.)

Fig. 5 Interaction between miR-1270 and LINC00094 in melanoma cells. **A** Venn diagram depicting the identification process of miR-1270, which was found to interact with LINC00094 through TargetScan prediction and to be upregulated in cells with LINC00094 knockdown along with si-LINC00094-2 and si-LINC00094-3 transfection through small RNA profiling. **B** Dual luciferase reporter assay indicating reduced relative luciferase activity of pMIR-REPROT-LINC00094 in cells cotransfected with miR-1270 mimics. **C**, **D** Ago2 precipitation assay indicating an interaction between miR-1270 and LINC00094 in the Ago2 complex. A375 cells were transfected with miR-1270 mimics for 48 h, followed by Ago2 protein precipitation. Real-time PCR was used to determine the expression levels of LINC00094 and miR-1270. **E**, **F** After transfection with siLINC00094 for 48 h, the expression levels of LINC00094 and miR-1270 were detected by real-time PCR. **G**, **H** After transfection with miR-1270 mimics for 48 h, the expression levels of LINC00094 and miR-1270 were detected by real-time PCR. $^{*}p < 0.05$; $^{**}p < 0.01$; $^{***}p < 0.001$

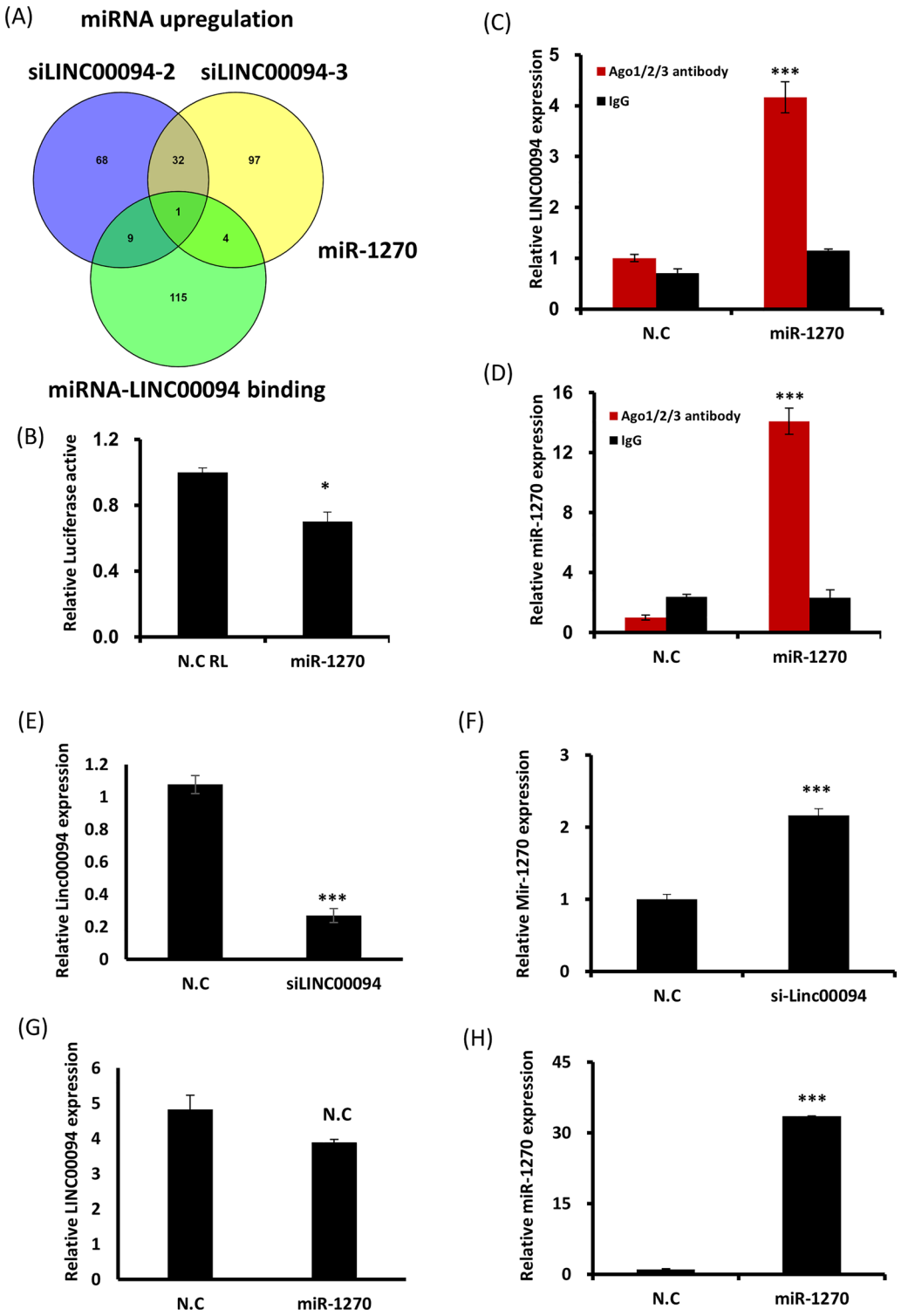

Fig. 5 (See legend on previous page.)

cancer to letrozole. In addition, LINC00094 upregulated the expression of CYP19A1, the target gene of miR-19a-3p, and inhibited the EMT process of breast cancer, ultimately increasing the sensitivity of ER-positive breast cancer cells to letrozole. Finally, Zhu et al. [58] discovered that the LINC00094/miR-224-5p (miR-497-5p)/

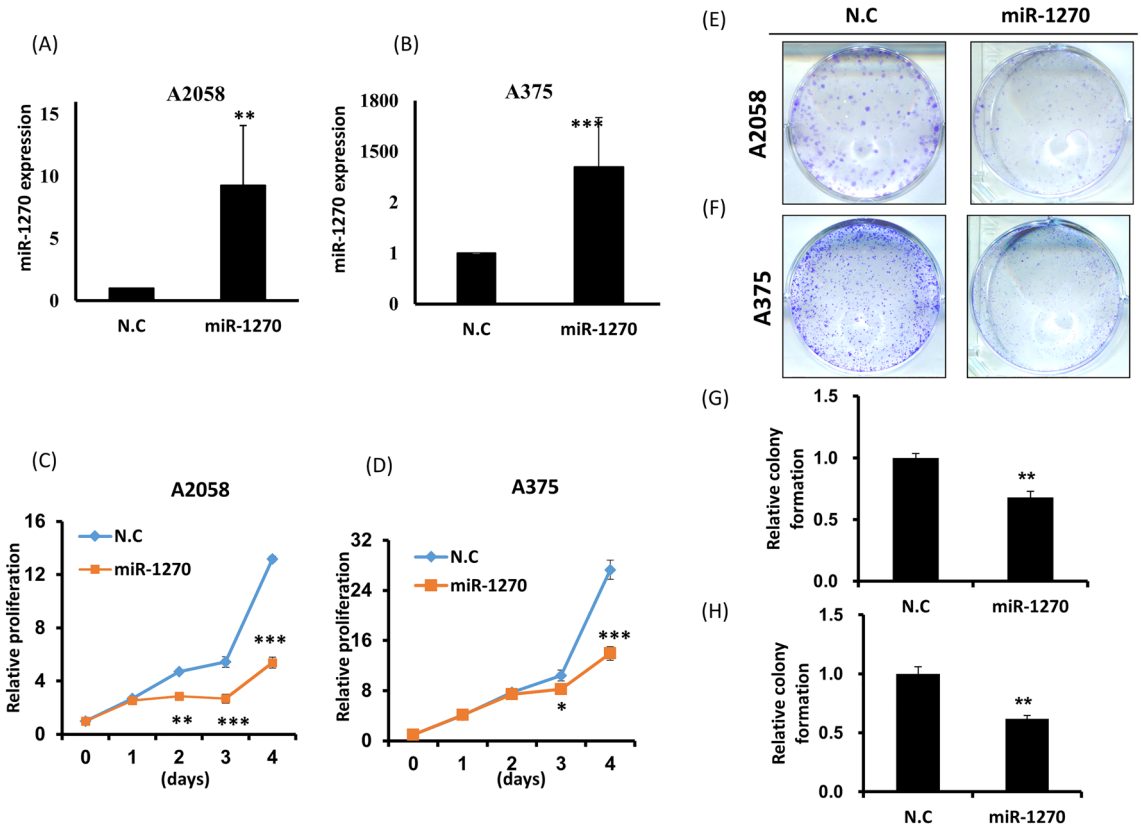

Fig. 6 Ectopic expression of miR-1270 inhibiting the growth of melanoma cells. **A**, **B** Evaluation of miR-1270 overexpression in A2058 and A375 cells transfected with mimics for 48 h through real-time PCR. **C**, **D** Evaluation of cell proliferation in A2058 and A375 cells transfected with miR-1270 mimics. **E**, **F** Examination of colony formation ability of A2058 and A375 cells after LINC00094 knockdown. **G**, **H** Quantification of relative colony formation ability

endophilin-1 axis in memantine had protective effects on the microenvironmental blood–brain barrier of patients with Alzheimer's disease.

Multiple studies have highlighted the importance of miR-1270. For instance, Zhao et al. [37] reported that miR-1270 modulated the expression of suppressor of cancer cell invasion (SCAI). That study also indicated that Cdr1as was downregulated in the serum exosomes of cisplatin-resistant patients with ovarian cancer and that circular RNA Cdr1as enhance SCAI to suppress cisplatin resistance in ovarian cancer through the inhibition of mir-1270. Yuan et al. [42] reported that circular RNA Cdr1as increased the sensitivity of bladder cancer to cisplatin by upregulating the expression of APAF1 through miR-1270 inhibition and the Cdr1as/miR-1270/APAF1 axis. That study also indicated that Cdr1as directly sponged miR-1270 and abolished its effect on APAF1. Luo et al. [41] reported that Circ-ZFR promoted the proliferation, migration, and invasion of bladder cancer cells by upregulating WNT5A through miR-545 and miR-1270 sponging. Wu et al. [59] discovered that knocking down cancer-promoting lncRNA SNHG8 inhibited the progression of esophageal cancer by regulating the miR-1270/BACH1 axis. Jin et al. [60] reported that engineered colorectal cancer (CRC) exosomes loaded with functional miR-1270 (Exo-miR-1270) strongly inhibited the proliferation and migration of CRC cells and promoted their apoptosis. That study also indicated that miR-1270 overexpression inhibited the growth of CRC cells in vivo and extended the OS of mice under safety evaluation. Song et al. [61] reported that lncRNA ASMTL-AS1 and miR-1270 are associated with poor prognosis in patients with gastric cancer. That study also indicated that ASMTL-AS1 inhibited the progression of gastric cancer by regulating miR-1270. Jiang et al. [39] reported that lncRNA KCNQ1OT1 mediated the progression of cervical cancer by sponging miR-1270 as a ceRNA of LOXL2 through the PI3K/AKT pathway. That study also indicated that the KCNQ1OT1/miR-1270/LOXL2 axis modulated the viability and apoptosis of cervical cancer cells. Finally, Chen et al. [36] reported that HCG11, a tumor suppressor, regulated the AKT/mTOR pathway and inhibited cell growth in ovarian cancer by modulating the miR-1270/PTEN pathway. That study also indicated that HCG11

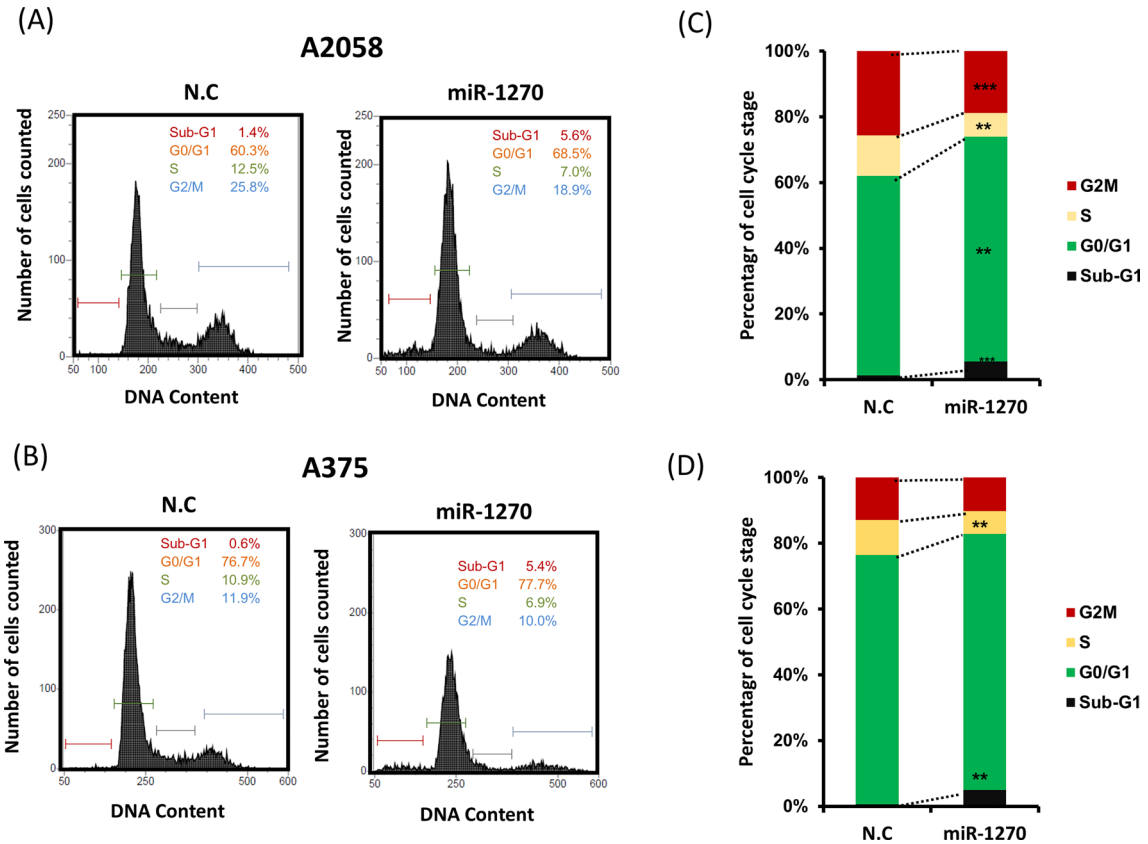

Fig. 7 Cell cycle in melanoma cells with miR-1270 mimic transfection. **A**, **B** A2058 and A375 cells transfected with miR-1270 mimics or scramble control (NC) for 2 days. After the cells had been stained with propidium iodide, cell cycle analysis was conducted using imaging flow cytometry. **C**, **D** Quantification of the percentage of cells in each cell cycle stage

was a promising target for the effective treatment of patients with ovarian cancer. However, the real relationship between miR-1270 and these target genes in melanoma remains unclear. In this study, two potential targets of miR-1270, CD276 and CENPM, were identified through in silico analysis. Both CD276 and CENPM may play oncogenic roles in melanoma progression. Chen et al. [62] identified CENPM as being involved in melanoma metastasis through an analysis of the GSE8401 microarray dataset from the Gene Expression Omnibus database. Their findings revealed that aberrant expression of CENPM was significantly associated with poor overall survival in melanoma patients. CD276, a member of the B7 family of immune regulatory proteins, is overexpressed in melanoma and is linked to worse survival outcomes [63]. Overexpression of CD276 enhances melanoma cell migration, invasion, and glycolysis, while its knockdown reduces these capabilities and increases sensitivity to chemotherapy [64, 65]. CD276 has also been found to modulate CD8+ T cell function in the melanoma tumor microenvironment [66]. High CD276 expression is associated with poor clinical outcomes, reduced tumor-infiltrating lymphocytes, and resistance to anti-PD-1 and anti-CTLA-4 immunotherapies for patients with melanoma [67].

Glycolysis (metabolic breakdown of glucose) is a process that drives catabolic ATP production through a pathway that couples the Krebs or tricarboxylic acid cycle with OXPHOS, which is a highly efficient pathway for chemical energy conversion in the mitochondria. Certain melanomas are associated with significantly higher oxygen consumption compared with melanocytes, indicating that OXPHOS may be an essential metabolic target in some tumors. Inhibition of OXPHOS induces apoptosis and drives enhanced glycolysis. Hence, melanomas depend on OXPHOS, and they can adapt to changes in metabolism [68]. BRAF mutations are a major regulator of metabolic homeostasis. Melanoma cells may undergo a metabolic shift to avoid BRAF-induced senescence by limiting their reliance on OXPHOS and by promoting proliferation. Therefore, therapeutic inhibition of BRAF reverses metabolic reprogramming in melanoma cells and promotes OXPHOS by increasing the levels of MITF-PGC1α [69].

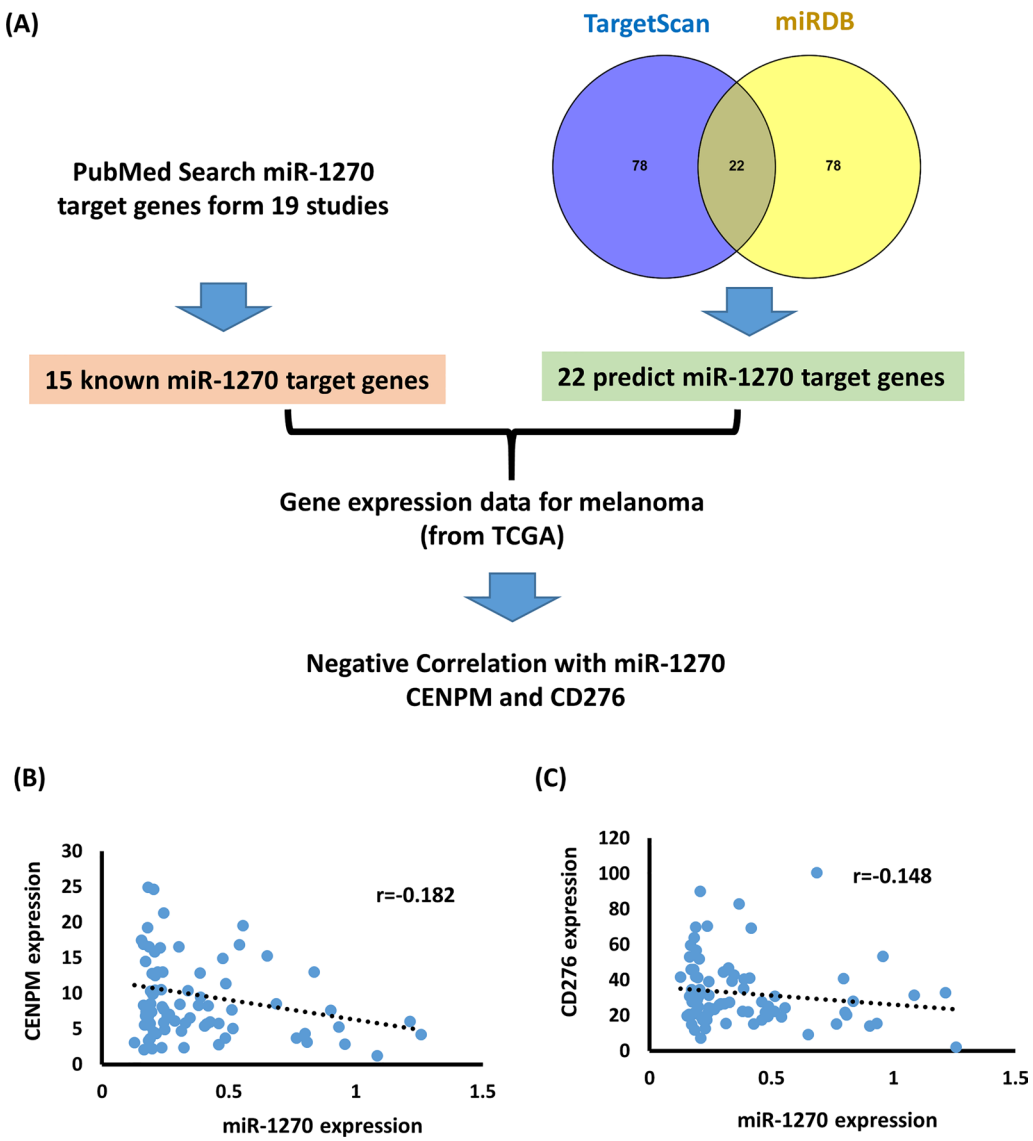

Fig. 8 In silico identification of miR-1270 target genes. **A** The flowchart illustrates the identification of miR-1270 target genes through a combination of literature search and target prediction approaches. Expression profiles for miR-1270 and its target genes in melanoma were obtained from the TCGA database. Pearson correlation coefficients were calculated for miR-1270 with CENPM (**B**) and CD276 (**C**)

BRAF oncogenes can drive and enhance the process of glycolysis. Changes in glycolysis, dysregulation in GAPDH expression, and activation of the PI3K/AKT/mTOR signaling pathway may substantially contribute to targeted therapy resistance for BRAF-mutated melanomas [70]. Upregulation of the PI3K/AKT/mTOR pathway is regarded as a bypass pathway in the therapeutic resistance of BRAF-mutated melanoma. In the absence of BRAF mutations, immune checkpoint inhibitors are typically used for the treatment of melanoma. By contrast, in the presence of BRAF mutations, targeted therapies are implemented with BRAF inhibitors (BRAFi) in combination with MEK inhibitors (MEKi). When patients with melanoma do not respond to these therapies, substitutive or bypass pathways, such as the upregulation of the PI3K/AKT/mTOR pathway, are activated. Therefore, combining BRAFi/MEKi and inhibitors of the PI3K/AKT/mTOR pathway may prevent the development of resistance [70]. In different melanoma cell lines, a high degree of diversity is often observed in how the PI3K pathway is activated. This PI3K pathway has been implicated as a target for melanoma therapy, with mTOR serving as an effective point for targeting growth through the PI3K pathway across all cell lines [71]. In

the case of MAPK/ERK independency, therapeutic focus may shift to the PI3K/AKT pathway to overcome late-stage resistance in melanoma tumors with a mesenchymal phenotype [72]. In this study, our data show that BRAF mutation status does not influence LINC00094 expression in melanoma. Furthermore, we identified CD276 and CENPM as a potential target gene of miR-1270, suggesting that the LINC00094/miR-1270 axis may provide new insights or play a crucial role in advancing immunotherapy.

Conclusion

In this study, we used NGS to identify metformin-regulated-miRNA/lncRNAs in melanoma cells. The role of LINC00094 is to regulate the growth melanoma cell by sponging miR-1270 expression and targeting genes of CD276 and CENPM. In addition, LINC00094 knockdown in A375 and A2058 cells inhibited mitochondrial function by regulating OXPHOS-related genes, antioxidant systems, ROS transcription factors, and glycolysis. Such knockdown also induced the downregulation of the PI3K-AKT pathway. Therefore, metformin treatment induced downregulation of LINC00094 can decreased the proliferation of melanoma cells.

LINC00094 is a key component of oncogenesis, influencing both growth and apoptosis by modulating cell cycle progression. This study introduced a novel mechanism emphasizing the importance of the LINC00094/miR-1270 axis in the therapeutic effect of metformin on melanoma. Overall, our findings underscore the therapeutic potential of targeting the LINC00094/miR-1270 axis for melanoma treatment, suggesting a promising avenue for future therapeutic interventions.

Supplementary Information

The online version contains supplementary material available at https://doi.org/10.1186/s12935-024-03545-5.

Figure S1. Next-generation sequencing was employed to analyze the expression profiles of melanoma cells treated with 5 mM metformin. (A) Summary of sequence reads in four libraries: the libraries included A2058 control (A2C), A2058 with metformin treatment (A2M), A375 control (A3C), and A375 with metformin treatment (A3M). (B) Volcano diagram illustrates the differential expression of lncRNAs in melanoma cells compared to the control group.

Figure S2. Gene structure of LINC00094 according to the UCSC human genome database. (A) The figure shows the locations of two siRNA sequences (si-LINC00094#2 and si-LINC00094#3) designed for LINC00094 knockdown. (B) The full-length LINC00094 sequence was cloned into the pCR4 TOPO vector. LINC00094 expression levels were measured by real-time PCR in A2058 cells with stable LINC00094 expression, compared to the control group. (C) After treatment with 5 mM metformin for 1 and 4 days, cell proliferation was assessed in A2058 cells with and without stable LINC00094 expression.

Figure S3. Involvement of LINC00094 in energy metabolic pathways. (A) Flowchart depicting the identification process of positively and negatively coexpressed genes with LINC00094 in TCGA. (B) The top 100 genes with positive and negative correlations were subjected to pathway enrichment analysis and gene ontology analysis in g:Profiler. (C) Genes coexpressed with LINC00094 were significantly enriched in mitochondrial OXPHOS signaling pathways.

Figure S4. Impact of BRAF mutation status on LINC00094 expression in melanoma. The expression levels of LINC00094 in melanoma were obtained from the TCGA database. BRAF mutation status in the same melanoma patients was retrieved from the cBioPortal database. LINC00094 expression levels were then compared between melanoma patients with BRAF wild-type and BRAF mutations.

Figure S5. Impairment of cell cycle and promotion of cell apoptosis by LINC00094 knockdown through the modulation of PI3K signaling activity. After siRNAs were transfected into A375 and A2058 cells for 48 h, the expression levels of (A) cell cycle, (B) PI3K, and (C) apoptosis proteins were examined using Western blotting.

Figure S6. Predominant expression of LINC00094 in the cytoplasm of melanoma cells. After nuclear and cytoplasmic fractionation, the expression levels of LINC00094 were examined using real-time PCR. U6 was used as a nuclear marker, and GAPDH was used as a cytoplasmic marker.

Supplementary Material 7.

Supplementary Material 8.

Supplementary Material 9.

Acknowledgements
The authors also thank the Core Laboratory of the Research Center in Taipei Tzu Chi Hospital and the Buddhist Tzu Chi Medical Foundation for their technical support and for allowing the authors access to their facilities.

Author contributions
KWT completed this study and drafted the manuscript. JBL conducted the IHC score and analysis. KWT and HWT supervised the study and edited the manuscript. All authors reviewed the manuscript.

Funding
This work was supported by funding from the Ministry of Science and Technology (MOST110-2314-B-075B-010, and MOST 111-2314-B-303-025), Taipei Tzu Chi Hospital, and the Buddhist Tzu Chi Medical Foundation (TCRD-TPE-MOST-111-15 and TCMF-CM3-112-03) and Kaohsiung Veterans General Hospital (VGHKS109-055).

Data availability
No datasets were generated or analysed during the current study.

Declarations

Consent for publication
All the authors have read and approved the final article.

Competing interests
The authors declare no competing interests.

Author details
[1]Department of Research, Taipei Tzu Chi Hospital, Buddhist Tzu Chi Medical Foundation, New Taipei City, Taiwan. [2]Department of Nursing, Cardinal Tien Junior College of Healthcare and Management, New Taipei City, Taiwan. [3]Department of Pathology and Laboratory Medicine, Kaohsiung Veterans General Hospital, Kaohsiung, Taiwan. [4]Shu Zen Junior College of Medicine and Management, Kaohsiung, Taiwan. [5]School of Medicine, College of Medicine, National Sun Yat-Sen University, Kaohsiung, Taiwan. [6]Department of Dermatology, Ministry of Health and Welfare Pingtung Hospital, Pingtung, Taiwan. [7]Institute of Biomedical Sciences, College of Medicine, National Sun Yat-Sen University, Kaohsiung, Taiwan. [8]School of Medicine, College of Medicine, National Sun Yat-Sen University, Kaohsiung, Taiwan. [9]Department of Nursing, College of Nursing, Meiho University, Neipu, Pingtung, Taiwan.

Received: 3 July 2024 Accepted: 22 October 2024
Published online: 19 November 2024

References

1. Siegel R, DeSantis C, Virgo K, Stein K, Mariotto A, Smith T, Cooper D, Gansler T, Lerro C, Fedewa S, et al. Cancer treatment and survivorship statistics, 2012. CA Cancer J Clin. 2012;62(4):220–41.
2. Miller AJ, Mihm MC Jr. Melanoma. N Engl J Med. 2006;355(1):51–65.
3. Florent L, Saby C, Slimano F, Morjani H. BRAF V600-mutated metastatic melanoma and targeted therapy resistance: an update of the current knowledge. Cancers. 2023;15(9):2607.
4. Rena G, Hardie DG, Pearson ER. The mechanisms of action of metformin. Diabetologia. 2017;60(9):1577–85.
5. Spizzo R, Almeida MI, Colombatti A, Calin GA. Long non-coding RNAs and cancer: a new frontier of translational research? Oncogene. 2012;31(43):4577–87.
6. Qu X, Alsager S, Zhuo Y, Shan B. HOX transcript antisense RNA (HOTAIR) in cancer. Cancer Lett. 2019;454:90–7.
7. Bhan A, Soleimani M, Mandal SS. Long noncoding RNA and cancer: a new paradigm. Can Res. 2017;77(15):3965–81.
8. Yu X, Zheng H, Tse G, Chan MT, Wu WK. Long non-coding RNAs in melanoma. Cell Prolif. 2018;51(4): e12457.
9. Liu P, Du R, Yu X. LncRNA HAND2-AS1 overexpression inhibits cancer cell proliferation in melanoma by downregulating ROCK1. Oncol Lett. 2019;18(2):1005–10.
10. Wang P, Hu L, Fu G, Lu J, Zheng Y, Li Y, Jia L. LncRNA MALAT1 promotes the proliferation, migration, and invasion of melanoma cells by downregulating miR-23a. Cancer Manag Res. 2020;12:6553–62.
11. Xia Y, Zhou Y, Han H, Li P, Wei W, Lin N. lncRNA NEAT1 facilitates melanoma cell proliferation, migration, and invasion via regulating miR-495-3p and E2F3. J Cell Physiol. 2019;234(11):19592–601.
12. Xu HL, Tian FZ. Clinical significance of lncRNA MIR31HG in melanoma. Eur Rev Med Pharmacol Sci. 2020;24(8):4389–95.
13. An LF, Huang JW, Han X, Wang J. Downregulation of lncRNA H19 sensitizes melanoma cells to cisplatin by regulating the miR-18b/IGF1 axis. Anticancer Drugs. 2020;31(5):473–82.
14. Guo J, Gan Q, Gan C, Zhang X, Ma X, Dong M. LncRNA MIR205HG regulates melanomagenesis via the miR-299-3p/VEGFA axis. Aging. 2021;13(4):5297.
15. Zhu L, Wang Y, Yang C, Li Y, Zheng Z, Wu L, Zhou H. Long non-coding RNA MIAT promotes the growth of melanoma via targeting miR-150. Hum Cell. 2020;33(3):819–29.
16. Han Y, Fang J, Xiao Z, Deng J, Zhang M, Gu L. Downregulation of lncRNA TSLNC8 promotes melanoma resistance to BRAF inhibitor PLX4720 through binding with PP1α to re-activate MAPK signaling. J Cancer Res Clin Oncol. 2021;147(3):767–77.
17. Li S, Sun X, Miao S, Liu J, Jiao W. Differential protein-coding gene and long noncoding RNA expression in smoking-related lung squamous cell carcinoma. Thorac Cancer. 2017;8(6):672–81.
18. Wang QY, Peng L, Chen Y, Liao LD, Chen JX, Li M, Li YY, Qian FC, Zhang YX, Wang F, et al. Characterization of super-enhancer-associated functional lncRNAs acting as ceRNAs in ESCC. Mol Oncol. 2020;14(9):2203–30.
19. Sun M, Liu X, Xia L, Chen Y, Kuang L, Gu X, Li T. A nine-lncRNA signature predicts distant relapse-free survival of HER2-negative breast cancer patients receiving taxane and anthracycline-based neoadjuvant chemotherapy. Biochem Pharmacol. 2020;189: 114285.
20. Zhang L, Wang Q, Wang L, Xie L, An Y, Zhang G, Zhu W, Li Y, Liu Z, Zhang X, et al. OSskcm: an online survival analysis webserver for skin cutaneous melanoma based on 1085 transcriptomic profiles. Cancer Cell Int. 2020;20:176.
21. Tseng HH, Tseng YK, You JJ, Kang BH, Wang TH, Yang CM, Chen HC, Liou HH, Liu PF, Ger LP, et al. Next-generation sequencing for microRNA profiling: microRNA-21-3p promotes oral cancer metastasis. Anticancer Res. 2017;37(3):1059–66.
22. Pan CT, Tsai KW, Hung TM, Lin WC, Pan CY, Yu HR, Li SC. miRSeq: a user-friendly standalone toolkit for sequencing quality evaluation and miRNA profiling. Biomed Res Int. 2014;2014: 462135.
23. Tseng HH, Chen YZ, Chou NH, Chen YC, Wu CC, Liu LF, Yang YF, Yeh CY, Kung ML, Tu YT, et al. Metformin inhibits gastric cancer cell proliferation by regulation of a novel Loc100506691-CHAC1 axis. Mol Ther Oncolytics. 2021;22:180–94.
24. Giraldez MD, Spengler RM, Etheridge A, Godoy PM, Barczak AJ, Srinivasan S, De Hoff PL, Tanriverdi K, Courtright A, Lu S, et al. Comprehensive multi-center assessment of small RNA-seq methods for quantitative miRNA profiling. Nat Biotechnol. 2018;36(8):746–57.
25. Tseng HW, Li SC, Tsai KW. Metformin treatment suppresses melanoma cell growth and motility through modulation of microRNA expression. Cancers. 2019;11(2):209.
26. Iijima T. Mitochondrial membrane potential and ischemic neuronal death. Neurosci Res. 2006;55(3):234–43.
27. Zhong S, Chen W, Wang B, Gao C, Liu X, Song Y, Qi H, Liu H, Wu T, Wang R, et al. Energy stress modulation of AMPK/$FoxO_3$ signaling inhibits mitochondria-associated ferroptosis. Redox Biol. 2023;63: 102760.
28. Nguyen TT, Wei S, Nguyen TH, Jo Y, Zhang Y, Park W, Gariani K, Oh CM, Kim HH, Ha KT, et al. Mitochondria-associated programmed cell death as a therapeutic target for age-related disease. Exp Mol Med. 2023;55(8):1595–619.
29. Gao N, Ye B. Circ-SOX4 drives the tumorigenesis and development of lung adenocarcinoma via sponging miR-1270 and modulating PLAGL2 to activate WNT signaling pathway. Cancer Cell Int. 2020;20:2.
30. Tai G, Fu H, Bai H, Liu H, Li L, Song T. Long non-coding RNA GLIDR accelerates the tumorigenesis of lung adenocarcinoma by miR-1270/TCF12 axis. Cell Cycle. 2021;20(17):1653–62.
31. Xiao Y, Najeeb RM, Ma D, Yang K, Zhong Q, Liu Q. Upregulation of CENPM promotes hepatocarcinogenesis through mutiple mechanisms. J Exp Clin Cancer Res. 2019;38(1):458.
32. Sun K, Wang H, Zhang D, Li Y, Ren L. Depleting circ_0088364 restrained cell growth and motility of human hepatocellular carcinoma via circ_0088364-miR-1270-COL4A1 ceRNA pathway. Cell Cycle. 2022;21(3):261–75.
33. Su Y, Lv X, Yin W, Zhou L, Hu Y, Zhou A, Qi F. CircRNA Cdr1as functions as a competitive endogenous RNA to promote hepatocellular carcinoma progression. Aging. 2019;11(19):8183–203.
34. Wei L, Li P, Zhao C, Wang N, Wei N. Upregulation of microRNA-1270 suppressed human glioblastoma cancer cell proliferation migration and tumorigenesis by acting through WT1. Onco Targets Ther. 2019;12:4839–48.
35. Liu Y, Guo W, Fang S, He B, Li X, Fan L. miR-1270 enhances the proliferation, migration, and invasion of osteosarcoma via targeting cingulin. Eur J Histochem. 2021;65(4):3237.
36. Chen X, Yang Y, Sun J, Hu C, Ge X, Li R. LncRNA HCG11 represses ovarian cancer cell growth via AKT signaling pathway. J Obstet Gynaecol Res. 2022;48(3):796–805.
37. Zhao Z, Ji M, Wang Q, He N, Li Y. Circular RNA Cdr1as upregulates SCAI to suppress cisplatin resistance in ovarian cancer via miR-1270 suppression. Mol Ther Nucleic Acids. 2019;18:24–33.
38. Yi T, Zhou X, Sang K, Zhou J, Ge L. MicroRNA-1270 modulates papillary thyroid cancer cell development by regulating SCAI. Biomed Pharmacother. 2019;109:2357–64.
39. Jiang L, Jin H, Gong S, Han K, Li Z, Zhang W, Tian J. LncRNA KCNQ1OT1-mediated cervical cancer progression by sponging miR-1270 as a ceRNA of LOXL2 through PI3k/Akt pathway. J Obstet Gynaecol Res. 2022;48(4):1001–10.
40. Wang W, Xu A, Zhao M, Sun J, Gao L. Circ_0001247 functions as a miR-1270 sponge to accelerate cervical cancer progression by up-regulating ZEB2 expression level. Biotechnol Lett. 2021;43(3):745–55.
41. Luo L, Miao P, Ming Y, Tao J, Shen H. Circ-ZFR promotes progression of bladder cancer by upregulating WNT5A via sponging miR-545 and miR-1270. Front Oncol. 2020;10: 596623.
42. Yuan W, Zhou R, Wang J, Han J, Yang X, Yu H, Lu H, Zhang X, Li P, Tao J, et al. Circular RNA Cdr1as sensitizes bladder cancer to cisplatin by upregulating APAF1 expression through miR-1270 inhibition. Mol Oncol. 2019;13(7):1559–76.
43. Tong Y, Zhou T, Wang X, Deng S, Qin L. Upregulation of CENPM promotes breast carcinogenesis by altering immune infiltration. BMC Cancer. 2024;24(1):54.
44. Zhou WT, Jin WL. B7–H3/CD276: an emerging cancer immunotherapy. Front Immunol. 2021;12: 701006.

45. Eddy K, Chen S. Overcoming immune evasion in melanoma. Int J Mol Sci. 2020;21(23):8984.
46. Tucci M, Passarelli A, Mannavola F, Felici C, Stucci LS, Cives M, Silvestris F. Immune system evasion as hallmark of melanoma progression: the role of dendritic cells. Front Oncol. 2019;9:1148.
47. Libby G, Donnelly LA, Donnan PT, Alessi DR, Morris AD, Evans JM. New users of metformin are at low risk of incident cancer: a cohort study among people with type 2 diabetes. Diabetes Care. 2009;32(9):1620–5.
48. Pernicova I, Korbonits M. Metformin—mode of action and clinical implications for diabetes and cancer. Nat Rev Endocrinol. 2014;10(3):143–56.
49. Kahn BB, Alquier T, Carling D, Hardie DG. AMP-activated protein kinase: ancient energy gauge provides clues to modern understanding of metabolism. Cell Metab. 2005;1(1):15–25.
50. Jaune E, Rocchi S. Metformin: focus on melanoma. Front Endocrinol. 2018;9:472.
51. Peppicelli S, Toti A, Giannoni E, Bianchini F, Margheri F, Del Rosso M, Calorini L. Metformin is also effective on lactic acidosis-exposed melanoma cells switched to oxidative phosphorylation. Cell Cycle. 2016;15(14):1908–18.
52. Urbonas V, Rutenberge J, Patasius A, Dulskas A, Burokiene N, Smailyte G. The impact of metformin on survival in patients with melanoma-national cohort study. Ann Epidemiol. 2020;52:23–5.
53. Montaudié H, Cerezo M, Bahadoran P, Roger C, Passeron T, Machet L, Arnault JP, Verneuil L, Maubec E, Aubin F, et al. Metformin monotherapy in melanoma: a pilot, open-label, prospective, and multicentric study indicates no benefit. Pigment Cell Melanoma Res. 2017;30(3):378–80.
54. Tomic T, Botton T, Cerezo M, Robert G, Luciano F, Puissant A, Gounon P, Allegra M, Bertolotto C, Bereder JM, et al. Metformin inhibits melanoma development through autophagy and apoptosis mechanisms. Cell Death Dis. 2011;2: e199.
55. Tian Y, Zhao L. Metformin induces apoptosis of melanoma B16 cells via PI3K/Akt/mTOR signaling pathways. J buon. 2020;25(4):2066–70.
56. Piipponen M, Riihilä P, Knuutila JS, Kallajoki M, Kähäri VM, Nissinen L. Super enhancer-regulated LINC00094 (SERLOC) upregulates the expression of MMP-1 and MMP-13 and promotes invasion of cutaneous squamous cell carcinoma. Cancers. 2022;14(16):3980.
57. Xiang Y, Liu H, Hu H, Li LW, Zong QB, Wu TW, Li XY, Fang SQ, Liu YW, Zhan Y, et al. LINC00094/miR-19a-3p/CYP19A1 axis affects the sensitivity of ER positive breast cancer cells to letrozole through EMT pathway. Aging. 2022;14(11):4755–68.
58. Zhu L, Lin M, Ma J, Liu W, Gao L, Wei S, Xue Y, Shang X. The role of LINC00094/miR-224-5p (miR-497-5p)/endophilin-1 axis in memantine mediated protective effects on blood-brain barrier in AD microenvironment. J Cell Mol Med. 2019;23(5):3280–92.
59. Wu Y, Liang Y, Li M, Zhang H. Knockdown of long non-coding RNA SNHG8 suppresses the progression of esophageal cancer by regulating miR-1270/BACH1 axis. Bioengineered. 2022;13(2):3384–94.
60. Jin Y, Sun L, Chen Y, Lu Y. The homologous tumor-derived-exosomes loaded with miR-1270 selectively enhanced the suppression effect for colorectal cancer cells. Cancer Med. 2024;13(1): e6936.
61. Song Z, Wang J. LncRNA ASMTL-AS1/microRNA-1270 differentiate prognostic groups in gastric cancer and influence cell proliferation, migration and invasion. Bioengineered. 2022;13(1):1507–17.
62. Chen J, Wu F, Shi Y, Yang D, Xu M, Lai Y, Liu Y. Identification of key candidate genes involved in melanoma metastasis. Mol Med Rep. 2019;20(2):903–14.
63. Wang J, Chong KK, Nakamura Y, Nguyen L, Huang SK, Kuo C, Zhang W, Yu H, Morton DL, Hoon DS. B7-H3 associated with tumor progression and epigenetic regulatory activity in cutaneous melanoma. J Invest Dermatol. 2013;133(8):2050–8.
64. Flem-Karlsen K, Tekle C, Øyjord T, Flørenes VA, Mælandsmo GM, Fodstad Ø, Nunes-Xavier CE. p38 MAPK activation through B7-H3-mediated DUSP10 repression promotes chemoresistance. Sci Rep. 2019;9(1):5839.
65. Erdrich J, Lourdault K, Judd A, Kaufman D, Gong KW, Gainsbury M, Deng N, Shon W, Essner R. Four immune modulating genes in primary melanoma that predict metastatic potential. J Surg Res. 2022;279:682–91.
66. Wu Y, Han W, Tang X, Liu J, Guo Z, Li Z, Cai C, Que L. B7–H3 suppresses CD8(+) T cell immunologic function through reprogramming glycolytic metabolism. J Cancer. 2024;15(9):2505–17.
67. Shen B, Mei J, Xu R, Cai Y, Wan M, Zhou J, Ding J, Zhu Y. B7-H3 is associated with the armored-cold phenotype and predicts poor immune checkpoint blockade response in melanoma. Pathol Res Pract. 2024;256: 155267.
68. Barbi de Moura M, Vincent G, Fayewicz SL, Bateman NW, Hood BL, Sun M, Suhan J, Duensing S, Yin Y, Sander C, et al. Mitochondrial respiration—an important therapeutic target in melanoma. PLoS ONE. 2012;7(8): e40690.
69. Haq R, Fisher DE, Widlund HR. Molecular pathways: BRAF induces bioenergetic adaptation by attenuating oxidative phosphorylation. Clin Cancer Res. 2014;20(9):2257–63.
70. Gambichler T, Harnischfeger F, Skrygan M, Majchrzak-Stiller B, Buchholz M, Müller T, Braumann C. In vitro experiments on the effects of GP-2250 on BRAF-mutated melanoma cell lines and benign melanocytes. Int J Mol Sci. 2023;24(20):15336.
71. Tran KB, Kolekar S, Jabed A, Jaynes P, Shih JH, Wang Q, Flanagan JU, Rewcastle GW, Baguley BC, Shepherd PR. Diverse mechanisms activate the PI 3-kinase/mTOR pathway in melanomas: implications for the use of PI 3-kinase inhibitors to overcome resistance to inhibitors of BRAF and MEK. BMC Cancer. 2021;21(1):136.
72. Corrales E, Levit-Zerdoun E, Metzger P, Mertes R, Lehmann A, Münch J, Lemke S, Kowar S, Boerries M. PI3K/AKT signaling allows for MAPK/ERK pathway independency mediating dedifferentiation-driven treatment resistance in melanoma. Cell Commun Signal. 2022;20(1):187.

Publisher's Note